A Bivalent Supramolecular GCP Ligand Enables Blocking of the Taspase1/Importin α Interaction

Alexander Höing[+],[a] Alexander Zimmermann[+],[b] Lisa Moews,[a] Matthias Killa,[b] Marius Heimann,[b] Astrid Hensel,[a] Jens Voskuhl,*[b] and Shirley K. Knauer*[a]

In memory of Prof. Dr. Carsten Schmuck (1968–2019)

Taspase1 is a unique protease not only pivotal for embryonic development but also implicated in leukemia as well as solid tumors. As such, it is a promising target in cancer therapy, although only a limited number of Taspase1 inhibitors lacking general applicability are currently available. Here we present a bivalent guanidiniocarbonyl-pyrrole (GCP)-containing supramolecular ligand that is capable of disrupting the essential interaction between Taspase1 and its cognate import receptor Importin α in a concentration-dependent manner *in vitro* with an IC_{50} of 35 μM. Here, size of the bivalent *vs* the monovalent construct as well as its derivation with an aromatic cbz-group arose as critical determinants for efficient interference of **2GC**. This was also evident when we investigated the effects in different tumor cell lines, resulting in comparable EC_{50} values (~40–70 μM). Of note, in higher concentrations, **2GC** also interfered with Taspase1's proteolytic activity. We thus believe to set the stage for a novel class of Taspase1 inhibitors targeting a pivotal protein-protein interaction prerequisite for its cancer-associated proteolytic function.

Due to its vastly diverse nature, cancer remains one of the most challenging diseases in the history of humankind. In 2018, 18.1 million people were diagnosed with cancer and it was the cause of death for 9.6 million.[1] While classical treatments involves surgery, radiotherapy and/or chemotherapy, the last becomes progressively limited due to the emergence of resistances.[2–3] Therefore, the development of new therapeutic approaches and novel anti-cancer drugs still remains an imperative task. There are many different proteins that are promising targets in anti-cancer therapies.[4–6] One of these is the protease Taspase1 (Threonine aspartase 1), a protein normally involved in embryonic developmental processes.[7–8] It is widely absent in adult, differentiated tissues, but re-expressed in many tumor cell lines. Although Taspase1 alone is not sufficient to transform cells, tumors become increasingly dependent on its presence.[9] Taspase1 is therefore classified as a "non-oncogene addiction protease". It was initially reported as the protease responsible for cleavage of the Mixed Lineage Leukemia protein (MLL), and its oncogenic fusion proteins.[7] Subsequently, more and more oncologically relevant proteins were identified as Taspase1 targets, including e.g. TFIIA (Transcription factor IIA) and USF2 (Upstream stimulatory factor 2), and the unconventional myosin Myo1F.[10–11] As a Taspase1 knock-out is moreover well tolerated in normal adult tissue, it is regarded as an immensely attractive drug target.[12]

In the last decades, several approaches have been presented or proposed to interfere with its enzymatic activity. Relevant strategies comprised substrate analogues, nanoparticles, as well as enforced dimerization of its two subunits.[13–15]

Nevertheless, none of those inhibitors has yet reached the clinics. Although Taspase1, together with the proteasome, belongs to the rather small class of threonine proteases, its catalytic activity is neither affected by common protease inhibitors nor by proteasome inhibitors.[7, 16]

As already indicated, Taspase1 is a very unique protease belonging to the type 2 asparaginase family of enzymes.[7] All members of this family share the ability to be autocatalytically processed in *cis*, but Taspase1 is the only family member that functions as a protease, cleaving other substrates by recognizing a conserved peptide motif with an aspartate at the P_1 position.[7,17–18] Referring to its rather complex activation process (Figure 1), Taspase1 is initially expressed as an inactive α/β-monomer (50 kDa).[7,17] Autoproteolysis into the two subunits α (28 kDa) and β (22 kDa) results in a proteolytically active heterodimer subsequently enabling cleavage of target proteins in *trans*.

Of note, mutation of the catalytic nucleophile, Thr234, not only results in loss of *cis*-activity and thus precludes formation of the two subunits, but also completely abolishes Taspase1's proteolytic function in *trans*.[7]

[a] *A. Höing,[+] L. Moews, Dr. A. Hensel, Prof. S. K. Knauer*
Institute for Molecular Biology II
Center for Medical Biotechnology (ZMB)
University of Duisburg-Essen
Universitätsstrasse 5, 45117 Essen (Germany)
E-mail: shirley.knauer@uni-due.de
[b] *A. Zimmermann,[+] M. Killa, M. Heimann, Prof. J. Voskuhl*
Faculty of Chemistry (Organic Chemistry) and CENIDE
University of Duisburg Essen
Universitätsstrasse 7, 45141 Essen (Germany)
E-mail: jens.voskuhl@uni-due.de
[+] *These authors contributed equally to this work.*

Supporting information for this article is available on the WWW under https://doi.org/10.1002/cmdc.202100640

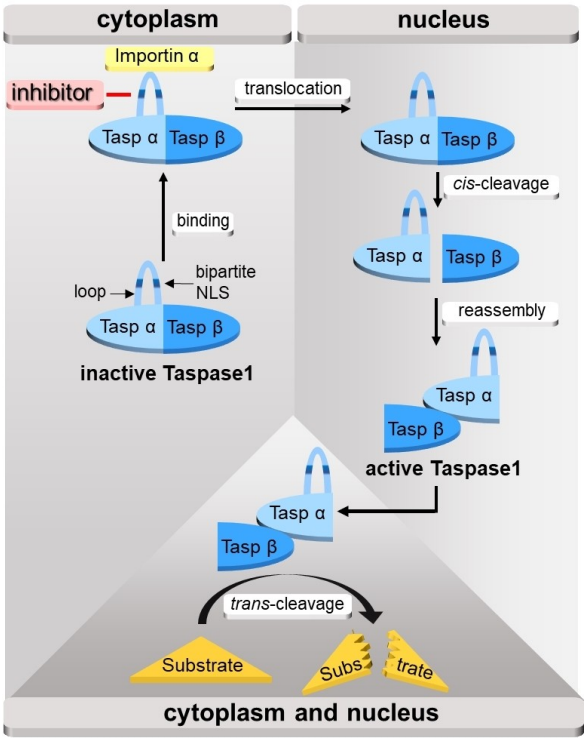

Figure 1. Cellular activation of Taspase1. The inactive Taspase1 proenzyme is synthesized in the cytoplasm, where it interacts with Importin α and is translocated into the nucleus. Here, Taspase1 is autoproteolytically processed into the α- and the β-subunit, re-assembling into a heterodimer enabling cleavage of cellular substrates in *trans*. Inhibition of this pivotal interaction (red line) should thus indirectly interfere with Taspase1's proteolytic function.

Moreover, the N-terminal part of the protein representing the α-subunit of Taspase1 contains a flexible loop region (aa178–233), consisting of two alpha helices.[19] These helices harbor a bipartite nuclear localization signal (NLS). As such, the latter comprises two basic amino acid clusters (^{197}KRNKRK^{202}, ^{217}KKRR^{220}) located in close proximity on the neighboring helices and thus constitute one single surface-accessible basic cluster.[17, 20]

This can be recognized by the adaptor protein Importin α, which might additionally recruit the carrier protein Importin β or solely transport Taspase1 into the nucleus.[20–21] Importantly, effective autoproteolysis into the two subunits *in vivo* requires a functionally intact NLS to efficiently interact with Importin α.[17] The Taspase1/Importin α interaction is thus regarded as an essential prerequisite to ensure full proteolytic activation.

Therefore, we aimed to develop cell-permeable molecules which target the respective protein binding interface using a structure-guided approach. Ligand design was based on the Schmuck binding motif guanidiniocarbonyl-pyrrole (GCP), generally suited for a wide range of applications in biomedical research.[22] It is used as protein recognition and modulation element but also serves as a pivotal component in transfection vectors[23–26] and as a building block in supramolecular polymers, gels and nanostructures.[22,27] Indeed, due to its function as a synthetic, and in comparison to its natural analogue arginine physiologically stable and thus superior recognition unit for oxo-anions,[24] the Schmuck binding motif is an ideal moiety to address protein surfaces in general, and in particular the rather flexible and completely surface-exposed loop region of Taspase1.[7,19,28–29] Here, a polycationic motif was chosen to primarily address negatively charged amino acids such as aspartic acid and glutamic acid present in this region. The Taspase1 loop adopts a helix-turn-helix conformation. Here, the amino acid sequence constituting the turn element indeed is the most exposed and accessible part of the loop. This turn region is rich in negatively charged amino acids, as well as a second surface-exposed stretch of negatively charged aspartic acid and glutamic acid in direct vicinity of the second helix.

To target both regions simultaneously, we decided to place two GCP units in a tandem arrangement to be tested in comprehensive biological assays (Figure 2). The compounds were synthesized by SPPS (Solid Phase Peptide Synthesis). The bivalent **2G** derivatives were obtained by dimerizing the corresponding monovalent **1G** derivatives with a 1,8-diaminooctane spacer connecting the (unprotected) lysins at first position of the G derivatives *via* two amide bonds (see Supporting Information for details, Figure S1, Table S1). Moreover, the protecting group of the second lysine was varied during SPPS to deduct potential effects of small structural changes. By introducing protecting groups like alloc (**A**) and cbz (**C**), the affinity of the structures with respect to hydrophobic amino acids such as valine or phenylalanine should be increased. The resulting ligands **2GA** and **2GC** might thus reveal an enhanced disruptive potency.

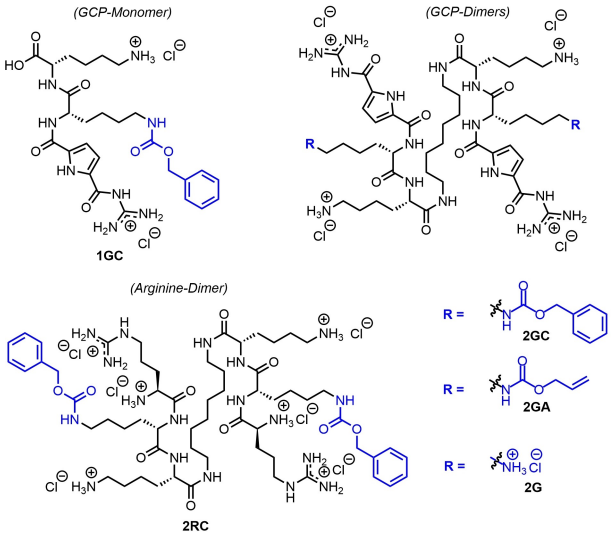

Figure 2. All compounds used in this study were synthesized by SPPS. **G** (GCP-containing-binding-unit) consist of two lysines and one GCP at the N-terminus (see Supporting Information for details, Figure S1–S22, Table S1). **G** was derivatized at the second lysine with a **C**(bz) or **A**(lloc) protecting group to generate the precursors for **2GC** and **2GA**. The bivalent compounds contain **2G** in a symmetric/palindromic arrangement with the sequence GCP-K(protected)-K-Spacer-K-K(protected)-GCP, harbouring the two unprotected lysines in the center. **2RC** represents a non-GCP containing bivalent control analogously equipped with two arginines (**R**) with two **C**(bz) protective groups.

First, we analysed the effects of our bivalent compounds on the Taspase1/Importin α interaction, utilizing a customized *in vitro* pull-down assay. Here, Importin α was recombinantly expressed with a N-terminal glutathione S-transferase (GST) affinity tag and immobilized on a glutathione sepharose-column to test for retention and thus binding of recombinant Taspase1-His protein subsequently applied to the column (see Supporting Information for details, Figure S26). Since wildtype Taspase1 partially undergoes autoproteolysis during protein purification, we used an inactive Taspase1 mutant unable to cleave in *cis* or *trans* (D233A/T234A).

Hereby, we assured homogeneity of the protein population required for an optimal reproducibility and robustness of our *in vitro* assay. Preceding pre-incubation of Taspase1 with either 100 μM of each compound or increasing concentrations of compound **2GC** (up to 100 μM) allowed to test the compound's inhibitory potential. Proteins were subsequently analysed by SDS-PAGE and immunoblotting with specific antibodies. Interestingly, **2GC** most efficiently interfered with the Taspase1/Importin α interaction (Figure 3A). Quantification of the pull-down data revealed an approx. 3-fold reduction; only 37% Taspase1 bound to column-immobilised Importin α compared to the untreated control. In contrast, the underivatized compound **2G** as well as the alloc derivative **2GA** showed no effect on the interaction, although both compounds differ from **2GC** only in the protecting group. Of note, routinely performed immunoblots of the unbound fractions revealed that column binding of Importin α was not affected by the ligands (Supporting Information Figure S27). Even more importantly, we synthesized the dimeric control compound **2RC**, bearing arginine (R) residues as generic cationic groups instead of the GCP moieties (see Supporting Information for details, Figure S2). In contrast to **2GC**, the arginine control **2RC** was not able to efficiently inhibit the interaction with Importin α (Supporting Information Figure S28).

Next, we performed molecular docking studies to shed more light on the binding mechanism of **2GC** (Figure 4, see Supporting Information for details, Figure S23–S25, Table S2). In contrast to a plethora of potential interactions of **2GC** and Taspase1 *via* hydrogen bonds, the hydrophobic cbz protecting group obviously does not take part in hydrogen bonding or electrostatic interactions with the protein but might be involved in hydrophobic interactions. However, **2GC** is suggested to

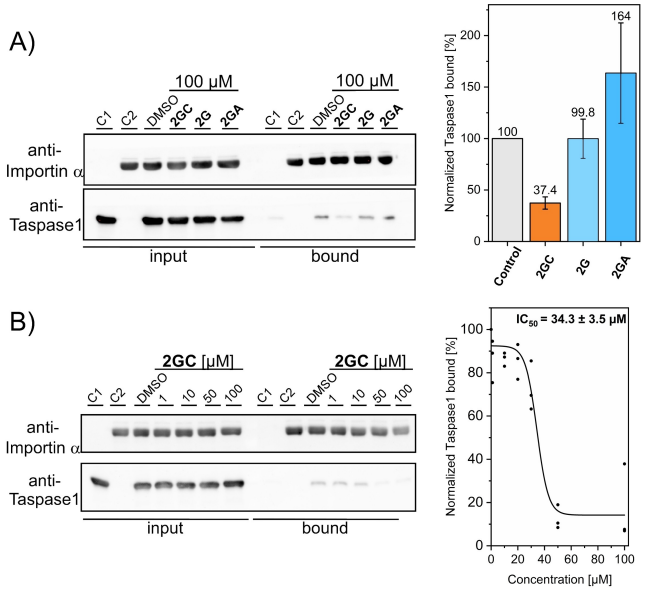

Figure 3. **2GC** effectively disrupts the interaction between Taspase1 and Importin α in a concentration-dependent manner. A) A specific pull-down setup allows to directly compare the effect of Taspase1 pre-incubation with 100 μM compound (**2GC**, **2G**, **2GA**). Controls include either only Taspase1 (C1), GST-Importin α (C2) or DMSO treatment. Quantification of results comprises the mean of three replicates ± standard deviation. B) By utilizing different concentrations of **2GC**, the pull-down assay reveals an IC_{50} of 34 ± 3.5 μM. Controls include only Taspase1 (C1) or GST-Importin α (C2). The results are the mean of three replicates ± standard deviation.

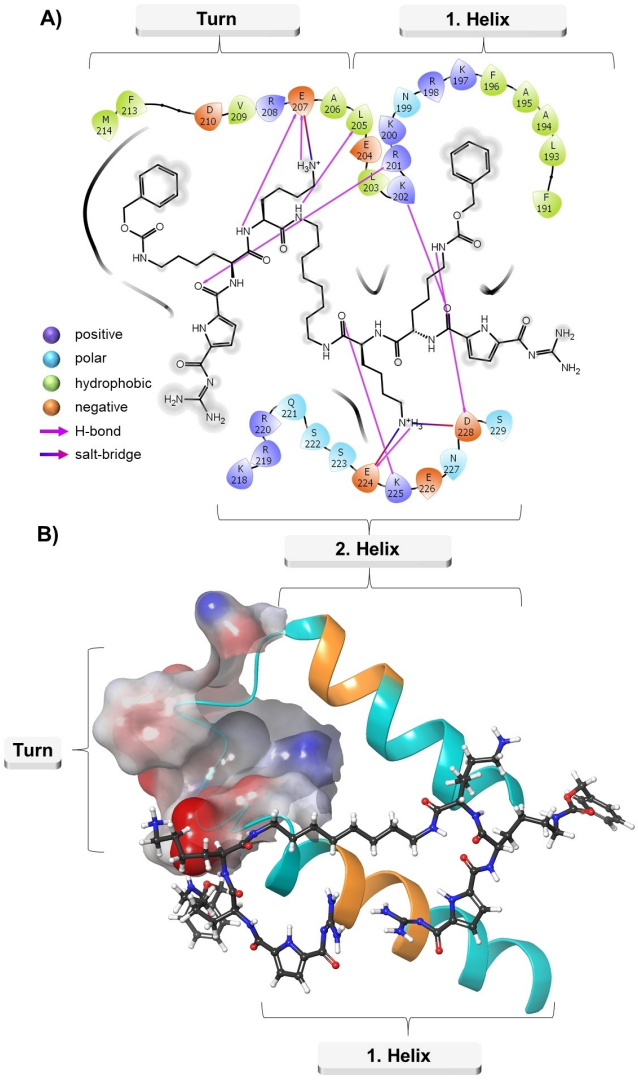

Figure 4. Modell of the interaction between **2GC** and the Taspase1 loop. A) LID of **2GC** and the loop sequence 189–229 aa. B) 3D model of **2GC** interacting with the loop. The latter consists of a helix(189–205 aa)-turn(206–215 aa)-helix(216–229 aa) motif, where basic amino acid clusters in both helices constitute the bipartite NLS (orange) that interacts with Importin α. The surface of the turn is rich in negative charged amino acids (red).

cover a large portion of the Taspase1 loop necessary for the interaction with the import receptor and thus might convey efficient steric shielding (Figure 4, Supporting Information Figure S25A/B).

We assume that the cbz protecting group might reveal an additional repulsive effect on Importin α, thus contributing to the observed inhibition of its interaction with Taspase1. Of note, although the docking scores of the GCP-containing compounds **2GC**, **2GA** and **1GC** were in the same order of magnitude, the score of **2RC** was less negative (Supporting Information Table S2), indicative for a decreased stabilizing energy. Comparative docking of **2RC** and **2GC** however revealed that similar areas were populated by the compounds, although **2GC** binds tighter and in a more closed conformation (Supporting Information Figure S24). This could hind towards a beneficial effect of the GCP unit compared to arginine at the same position.

We were subsequently focusing on **2GC** as the so far most effective compound. However, an exact quantification of pull-down experiments is not trivial and rather allows to determine an order of magnitude instead of discrete binding parameters. However, by rationally adapting the concentration range we acquired sufficient data points for a robust fit and could finally determine an IC_{50} of 34 ± 3.5 μM for its disruptive effect observed in our pull-down setup (Figure 3B). To further underscore our bivalent design concept, we also compared **2GC** to its monovalent counterpart **1GC**. As hypothesized, the prominent effect of **2GC** (quantification revealed 23% Taspase1 bound) could not be retained using the equally derivatized monovalent building block **1GC** (79% Taspase1 bound as revealed by quantification) in the pull-down assay (Figure 5). This strongly indicates that the molecular surface size is indeed important to mediate efficient interference with the interaction between Taspase1 and Importin α. Interestingly, molecular docking studies demonstrated that **1GC** is also able to interact with different Taspase1 amino acid residues (Supporting Information Figure S25D). However, **1GC** is not supposed to interact with the bipartite NLS inside the loop that is necessary for the interaction with Importin α, explaining its impaired potency.

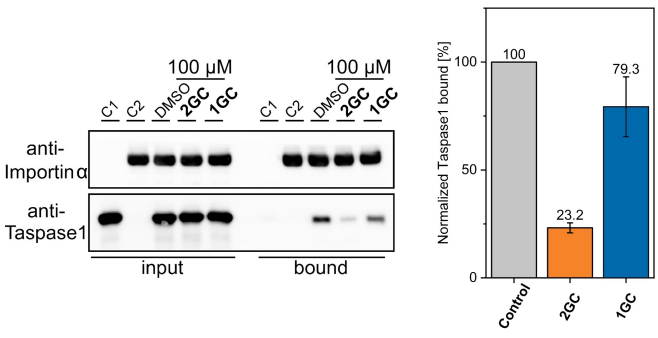

Figure 5. Only the bivalent but not the monovalent compound allows to efficiently interfere with the Taspase1/Importin α interaction. In our pull-down setup, pre-incubation Taspase1 with **2GC** hampers binding to column-bound Importin α in contrast to **1GC**. Controls include either only Taspase1 (C1), GST-Importin α (C2) or DMSO treatment (DMSO). Quantification of results comprises the mean of three replicates ± standard deviation.

The 3D model also indicates that **1GC** might not be able to shield an area of sufficient dimension to efficiently interfere with the Taspase1/Importin α interaction (Supporting Information Figure S25C).

As the residues targeted by **2GC** are in close proximity to Taspase1's active site, we further aimed to analyse whether **2GC** also affects its proteolytic activity. Therefore, we newly established a robust, *semi-in vitro* Taspase1 substrate cleavage assay (see Supporting Information for details, Figure S29). Here, we used 293T cells which express only neglectable amounts of endogenous Taspase1 to only rely on the activity of defined amounts of recombinant, fully active Taspase1-His to the cell lysates. As a confirmed Taspase1 substrate, we decided for the transcription factor USF2 (Upstream stimulatory factor 2),[10] which was overexpressed in cell culture. Respective cell lysates were incubated with recombinant Taspase1-His in the absence or presence of 500 μM of each compound for 4 h and 6 h. Indeed, immunoblot analysis revealed an inhibitory effect of **2GC** on Taspase1-mediated USF2 cleavage, which could not be evidenced for compounds **1GC**, **2GA**, **2G** (Supporting Information Figure S30A) or **2RC** (Supporting Information Figure S31), irrespective of the incubation time. Next, we stepwise decreased the concentration of **2GC** from 500 μM down to 100 μM. However, **2GC** was only effective up to 400 μM (Supporting Information Figure S30B). As in this assay the use of cell lysates supersedes the necessity of nuclear translocation as a prerequisite for Taspase1 activation, the observed effect could not be attributed to the compound's ability to interfere with Importin α binding. Moreover, the high concentration of the compound needed to affect Taspase1's proteolytic activity rather indicates the occupation of a neighbouring, least favoured region in the flexible loop. However, we next indeed investigated the effect of our compounds *in vivo* using two different Taspase1-expressing tumor cell lines, namely the cervical carcinoma cell line HeLa and the lung cancer cell line A549. Cells were incubated with different compound concentrations for 24 h, and toxicity was determined utilizing a colorimetric MTS assay for the quantification of viable cells. Indeed, **2GC** decreased the viability of HeLa ($EC_{50} = 69.9 \pm 1.8$ μM) and A549 ($EC_{50} = 40.9 \pm 8.2$ μM) cells (Figure 6A, B, Supporting Information Figure S32A). In contrast, the compounds **2GA**, **2G**, **1GC** and **2RC** had a rather negligible *in vivo* effect, even when applied in concentrations of 100 μM or even above (Figure 6, Supporting Information Figure S32B–E). Although this is still no airtight proof that Taspase1 is indeed responsible for the observed effect, these results are congruent with those achieved in the pull-down assays (Figure 3A, B, Figure 5).

In sum, our results demonstrate the feasibility of targeting the Taspase1-Importin α interaction with symmetry-based GCP-containing ligands. Ligand docking simulations by molecular force field calculations indicate that **2GC** might act as a symmetric clamp grasping the Taspase1 loop at its turning point and thus shield the NLS by steric hindrance. This results in an effective disruption of the Taspase1/Importin α interaction substantiated by *in vitro* pull-down assays.

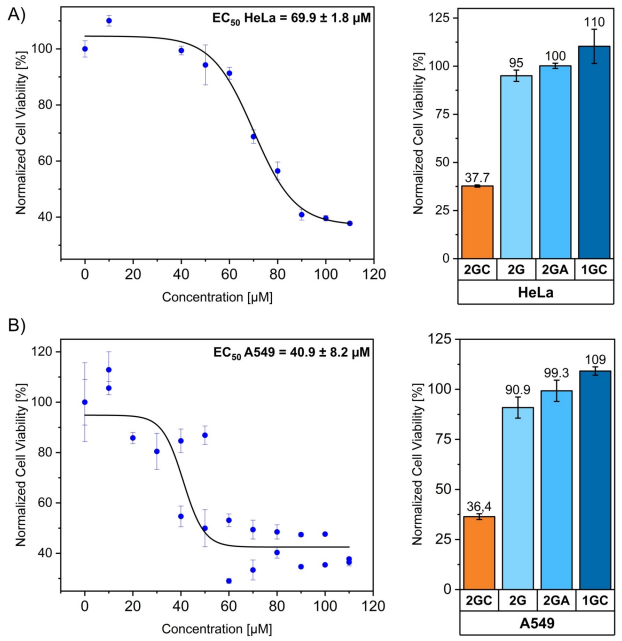

Figure 6. 2GC affects the viability of tumor cells. A) Determination of the EC_{50} value of **2GC** in HeLa cells ($EC_{50} = 69.9 \pm 1.8$ µM). In contrast to **2GC**, **2G**, **2GA** and **1GC** do not impair tumor cell viability even at the maximal concentration of 110 µM. Each data point is the mean of three replicates ± standard deviation. B) Determination of the EC_{50} value of **2GC** in A549 cells ($EC_{50} = 40.9 \pm 8.2$ µM). In contrast to **2GC**, **2G**, **2GA** and **1GC** do not impair tumor cell viability even at the maximal concentration of 110 µM. To allow a more robust curve fitting, results of two experiments were combined. Each data point is the mean of three replicates ± standard deviation.

Moreover, a *semi*-in vitro Taspase1 substrate cleavage assay also showed that the enzyme activity of Taspase1 is affected by **2GC**, albeit in rather high micromolar concentrations. Finally, we could demonstrate an anti-proliferative effect of **2GC** in Taspase1-expressing tumor cell lines.

However, further studies are now required to deeply investigate the binding kinetics and the mechanism underlying the effect on cell viability.

In conclusion, we developed a bivalent supramolecular GCP ligand that effectively targets the interaction between Taspase1 and Importin α, which is essential for its proteolytic activation. This now sets the stage for the development of a novel class of inhibitors targeting this therapeutically relevant protease.

Acknowledgements

This work was supported by the DFG collaborative research centre1093 (CRC 1093 – Projects A1, A10 and B5). Open Access funding enabled and organized by Projekt DEAL.

Conflict of Interest

The authors declare no conflict of interest.

Keywords: Taspase1 · Importin α · protein-interaction · nuclear localization signal (NLS) · protease · substrate cleavage assay · SPPS · supramolecular inhibition

[1] World Health Organization: Regional Office for Europe, *World Cancer Report: Cancer Research for Cancer Prevention*, IARC, **2020**.
[2] F. McCormick, *Nat. Rev. Cancer.* **2001**, *1*, 130–141.
[3] N. Vasan, J. Baselga, D. M. Hyman, *Nature* **2019**, *575*, 299–309.
[4] J. L. Delgado, C.-M. Hsieh, N.-L. Chan, H. Hiasa, *Biochem. J.* **2018**, *475*, 373–398.
[5] Q. Li, W. Xu, *Curr. Med. Chem. Anti-Cancer Agents* **2005**, *5*, 53–63.
[6] B. Kumar, S. Singh, I. Skvortsova, V. Kumar, *Curr. Med. Chem.* **2017**, *24*, 4729–4752.
[7] J. J.-D. Hsieh, E. H.-Y. Cheng, S. J. Korsmeyer, *Cell* **2003**, *115*, 293–303.
[8] D. Y. Chen, Y. Lee, B. A. van Tine, A. C. Searleman, T. D. Westergard, H. Liu, H.-C. Tu, S. Takeda, Y. Dong, D. R. Piwnica-Worms, K. J. Oh, S. J. Korsmeyer, A. Hermone, R. Gussio, R. H. Shoemaker, E. H.-Y. Cheng, J. J.-D. Hsieh, *Cancer Res.* **2012**, *72*, 736–746.
[9] D. Y. Chen, H. Liu, S. Takeda, H.-C. Tu, S. Sasagawa, B. A. van Tine, D. Lu, E. H.-Y. Cheng, J. J.-D. Hsieh, *Cancer Res.* **2010**, *70*, 5358–5367.
[10] C. Bier, S. K. Knauer, A. Klapthor, A. Schweitzer, A. Rekik, O. H. Kramer, R. Marschalek, R. H. Stauber, *J. Biol. Chem.* **2011**, *286*, 3007–3017.
[11] S. Takeda, S. Sasagawa, T. Oyama, A. C. Searleman, T. D. Westergard, E. H. Cheng, J. J. Hsieh, *J. Clin. Invest.* **2015**, *125*, 1203–1214.
[12] S. Takeda, D. Y. Chen, T. D. Westergard, J. K. Fisher, J. A. Rubens, S. Sasagawa, J. T. Kan, S. J. Korsmeyer, E. H.-Y. Cheng, J. J.-D. Hsieh, *Genes Dev.* **2006**, *20*, 2397–2409.
[13] J. van den Boom, A. Hensel, F. Trusch, A. Matena, S. Siemer, D. Guel, D. Docter, A. Hoing, P. Bayer, R. H. Stauber, S. K. Knauer, *Nanoscale* **2020**, *12*, 19093–19103.
[14] J. van den Boom, M. Mamic, D. Baccelliere, S. Zweerink, F. Kaschani, S. Knauer, P. Bayer, M. Kaiser, *ChemBioChem* **2014**, *15*, 2233–2237.
[15] C. Bier, S. K. Knauer, D. Wünsch, L. Kunst, S. Scheiding, M. Kaiser, C. Ottmann, O. H. Krämer, R. H. Stauber, *FASEB J.* **2012**, *26*, 3421–3429.
[16] M. Bochtler, L. Ditzel, M. Groll, C. Hartmann, R. Huber, *Annu. Rev. Biophys. Biomol. Struct.* **1999**, *28*, 295–317.
[17] C. Bier, S. K. Knauer, D. Docter, G. Schneider, O. H. Kramer, R. H. Stauber, *Traffic* **2011**, *12*, 703–714.
[18] D. Wünsch, A. Hahlbrock, S. Jung, T. Schirmeister, J. van den Boom, O. Schilling, S. K. Knauer, R. H. Stauber, *Oncogene* **2016**, *35*, 3351–3364.
[19] J. van den Boom, F. Trusch, L. Hoppstock, C. Beuck, P. Bayer, *PLoS One* **2016**, *11*, e0151431, 1–13.
[20] A. Lange, R. E. Mills, C. J. Lange, M. Stewart, S. E. Devine, A. H. Corbett, *J. Biol. Chem.* **2007**, *282*, 5101–5105.
[21] Y. Miyamoto, K. Yamada, Y. Yoneda, *J. Biochem.* **2016**, *160*, 69–75.
[22] M. Giese, J. Niemeyer, J. Voskuhl, *ChemPlusChem* **2020**, *85*, 985–997.
[23] C. Vallet, D. Aschmann, C. Beuck, M. Killa, A. Meiners, M. Mertel, M. Ehlers, P. Bayer, C. Schmuck, M. Giese, S. K. Knauer, *Angew. Chem. Int. Ed.* **2020**, *59*, 5567–5571; *Angew. Chem.* **2020**, *132*, 5614–5619.
[24] L. Bartsch, M. Bartel, A. Gigante, J. Iglesias-Fernández, Y. B. Ruiz-Blanco, C. Beuck, J. Briels, N. Toetsch, P. Bayer, E. Sanchez-Garcia, C. Ottmann, C. Schmuck, *ChemBioChem* **2019**, *20*, 2921–2926.
[25] M. Li, S. Schlesiger, S. K. Knauer, C. Schmuck, *Angew. Chem. Int. Ed.* **2015**, *54*, 2941–2944; *Angew. Chem.* **2015**, *127*, 2984–2987.
[26] D. Maity, A. Gigante, P. A. Sanchez-Murcia, E. Sijbesma, M. Li, D. Bier, S. Mosel, S. Knauer, C. Ottmann, C. Schmuck, *Org. Biomol. Chem.* **2019**, *17*, 4359–4363.
[27] G. Gröger, W. Meyer-Zaika, C. Böttcher, F. Gröhn, C. Ruthard, C. Schmuck, *J. Am. Chem. Soc.* **2011**, *133*, 8961–8971.
[28] C. Schmuck, *Chem. Commun.* **1999**, 843–844.
[29] C. Schmuck, L. Geiger, *Curr. Org. Chem.* **2003**, *7*, 1485–1502.

Manuscript received: October 1, 2021
Accepted manuscript online: October 8, 2021
Version of record online: October 19, 2021